CHEMISTRY OF MATERIALS

pubs.acs.org/cm

Methods/Protocols

In Situ Methods for Metal-Flux Synthesis in Inert Environments

Ashley Weiland, Matthew G. Frith, Saul H. Lapidus,* and Julia Y. Chan*

Cite This: *Chem. Mater.* 2021, 33, 7657−7664

Read Online

ACCESS | Metrics & More | Article Recommendations | Supporting Information

ABSTRACT: Flux growth synthesis is an advantageous synthetic method as it allows for the growth of single crystals of both congruently melting and metastable phases. The determination of synthetic parameters for the flux growth of new crystalline phases is complex as many factors and parameters need to be considered, such as the purity and morphology of the starting material and heating profile variables including maximum temperature, dwell time, cooling rate, and flux removal temperature. In situ monitoring of crystallite growth can lead to elucidation of reaction intermediates and growth mechanisms. The determination of pivotal reaction parameters can revolutionize the way growth parameters are selected. Herein, we report a new sample environment and furnace apparatus for synchrotron in situ synthesis of crystalline materials, including flux grown intermetallics.

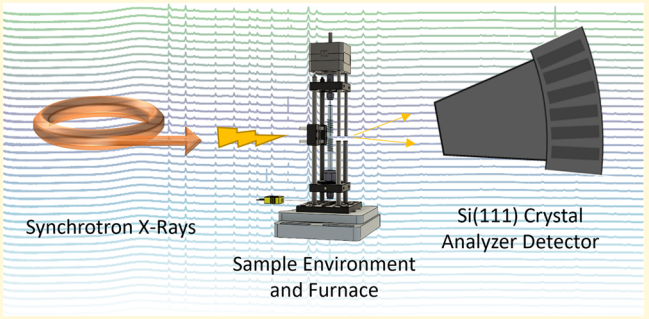

INTRODUCTION

In 2014, Shoemaker et al. published a groundbreaking way to study the formation of solid state phases with temperature dependent in situ X-ray diffraction studies.[1] Simultaneous heat treatment and characterization of inorganic precursors with salt fluxes led to the discovery of previously unknown phases, including phases that would not have been recovered ex situ. For example, the investigation of Cu or Sn with K_2S_3 or K_2S_5 as a flux led to the discovery of previously unknown intermediate phases such as $K_3Cu_4S_4$, $K_6Sn_2S_7$, $K_4Sn_2S_6$, and $K_5Sn_2S_8$. Additionally, the identification of reaction intermediates[2,3] creates an opportunity to ascertain reaction mechanisms and determine the formation of polymorphs.[4−6] Phase identification at different stages during the synthesis can guide tailored temperature profiles.[1,7−12] In addition, in situ high temperature powder diffraction methods coupled with the fast hydride route led to the discovery of new ternary phases in the Na−Zn−Sb system including $NaZn_4Sb_{33}$ and related $Na_{1-x}Zn_{4-y}Sb_3$.[13] Neutron diffraction in situ studies have also proven useful. For example, the optimization of the growth of $Cu_{22}Fe_8Ge_4S_{32}$ and other related complex chalcogenides[14] and the flux growth of Ba/Yb/Mg/Si phases revealed a lack of precipitation or interconversion of phases during crystal growth. Rather, each phase can be targeted by adjusting the reaction cooling rate: $Ba_5Yb_2Mg_{17}Si_{12}$ forms when slowly cooled to 800 °C and $Ba_{20}Yb_5Mg_{61}Si_{43}$ forms when fast cooled to 640 °C.[15]

In addition to phase formation, other factors can be monitored via in situ studies to further understand physical phenomena, including phase stability,[16,17] structural integrity,[18,19] and property evolution including in situ transport[20] and electrochemical[21] and thermoelectric properties.[22] For example, quantitative studies regarding the impact of annealing temperatures and cooling conditions provided insight into the dynamics of order/disorder phase transitions in the Pt_3Co nanoparticle catalysts.[23]

Determining the most suitable reaction profile for the synthesis of extended solids is complex as numerous multifaceted factors must be considered.[24−33] Binary phase diagrams can initially serve as a guide in determining heating profiles, but growing single crystals of ternary compounds presents a challenge given the additional intensive thermodynamic variables. While the mechanisms driving the formation of solid state phases are still largely unknown, the flux growth method is critical for the synthesis of exotic extended solids as single crystals.[25,29,30,34−36] Challenges associated with the growth of extended solids include the selection of the most suitable starting materials in addition to a compatible low-melting flux. Factors such as purity and morphology of the starting material, e.g., grain size of powders, chunks, or pellets, should be considered in relation to reactivity. The reaction vessel must be appropriate for the synthetic conditions and not be reactive with the elements.[25,30,34] The development of successful heating profiles relies on many kinetic and thermodynamic factors which must be considered, such as maximum temperature, dwell time, cooling rate, and flux removal temperature. The most important variable for a

Received: July 12, 2021
Revised: September 11, 2021
Published: September 22, 2021

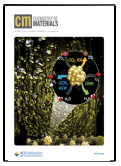

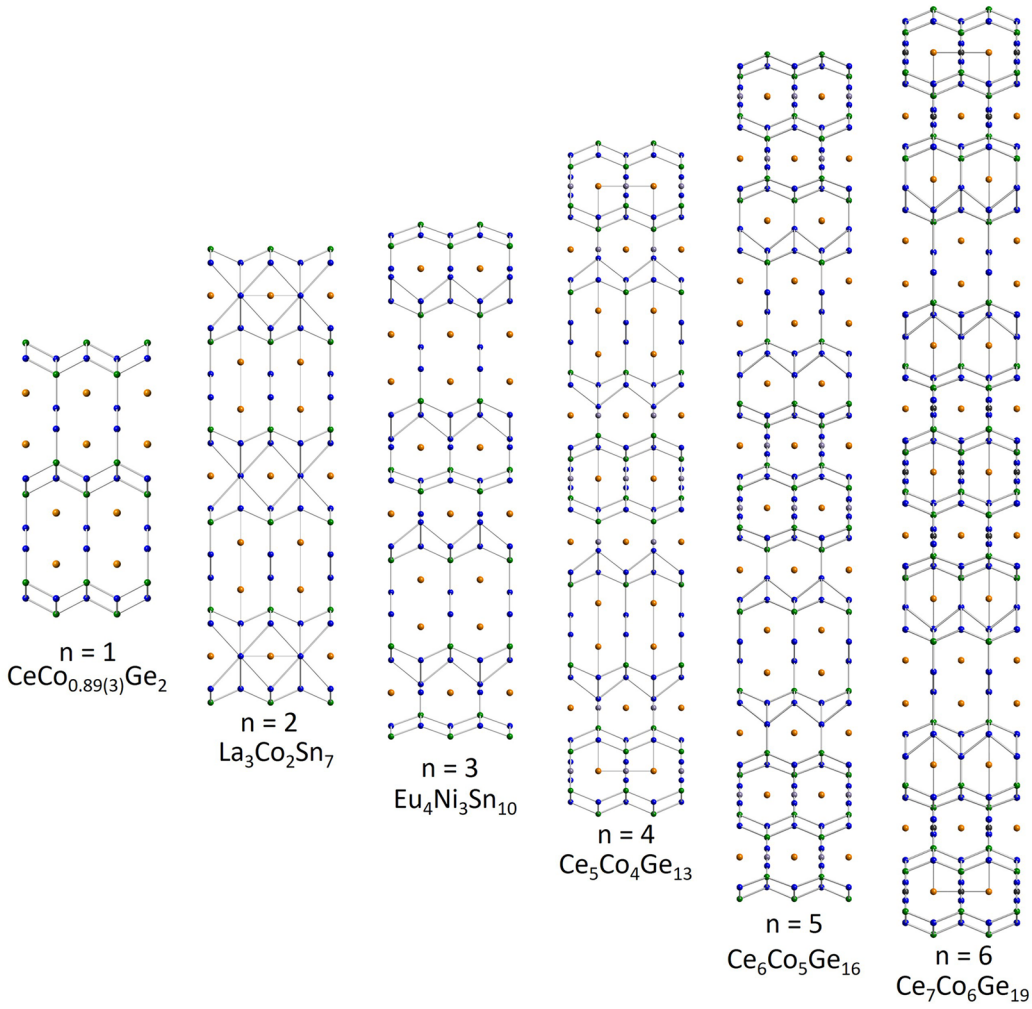

Figure 1. $A_{n+1}M_nX_{3n+1}$ (A = rare earth; M = transition metal; X = tetrels; n = 1−6) homologous series where increasing n correlates to increased stacking of subunits along the b axis.

successful targeted reaction is dependent on the material being investigated. The current approach to selecting reaction conditions for intermetallics is based on chemical intuition and guided/biased previous experiments of related phases. Once the reaction is completed, which can take between a few days to a few weeks, the products are removed and characterized. Without in situ data to guide temperature profile selection, new growth conditions are modified/optimized based on the identity and purity of the final products. Therefore, the synthetic understanding of the growth processes of both stable and metastable materials are necessary for targeted synthesis of new high-quality materials.

$Ce_{n+1}Co_nGe_{3n+1}$ HOMOLOGOUS SERIES

In light of the recent discovery of an intermetallic homologous series, $Ce_{n+1}Co_nGe_{3n+1}$ (Figure 1),[37] and the accompanying challenges to grow each member, it became necessary to determine synthetic parameters to grow and characterize each member of the series (n = 1−6). Single crystals of $Ce_6Co_5Ge_{16}$ and $Ce_7Co_6Ge_{19}$[38,39] were first grown with Ce:Co:Ge with >10-fold excess flux, typically by heating to 1100 °C for an average of 3−5 days before slow cooling to 815 °C. Due to the similarity in the compositions for the members of the homologous series, exclusive growth of the individual phases has not yet been achieved. Therefore, we set forth to utilize the high resolution synchrotron beamline 11-BM at the Advanced Photon Source at Argonne National Laboratory[40] to implement in situ studies in the growth of the intermetallic series. To monitor reaction evolution and phase formation, we were motivated to design an in situ apparatus suitable to withstand the necessary reaction conditions. Designing in situ experiments is nontrivial. Each experimental parameter, from equipment to synthetic variables, must be carefully considered to optimize monitorization. Additionally, new aspects such as time, temperature, scale, and absorption need to be considered. Once data is collected, determining phases present and point of formation can be arduous. Multiple phases and new phases present will complicate deconvolution and analysis of the powder pattern. This work describes a new sample environment and puts forth a methodology to perform in situ X-ray diffraction measurements for solid-state syntheses, specifically for air sensitive, metal flux intermetallic reactions. Furthermore, rational steps and considerations are discussed to help others prepare for in situ work.

https://doi.org/10.1021/acs.chemmater.1c02413
Chem. Mater. 2021, 33, 7657−7664

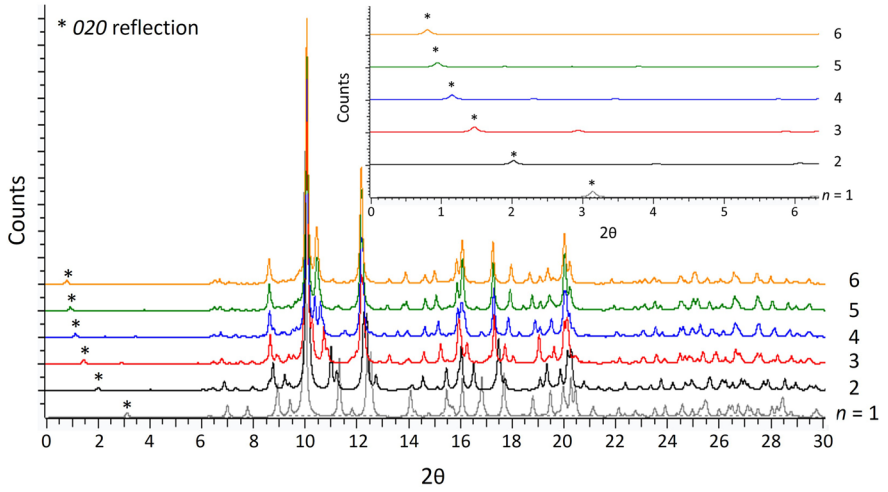

Figure 2. Simulated powder patterns (λ = 0.4592 Å) for n = 1−6 members of the $Ce_{n+1}Co_nGe_{3n+1}$ homologous series. The 020 low angle reflection is marked with an * to highlight the long b lattice parameter.

IN SITU SYNTHETIC CONSIDERATIONS

There are seven primary questions that need to be addressed before preforming an in situ experiment, which will be outlined below.

Question 1: What Beamline Should You Use? The beamline chosen for the experiments will dictate the answers to the following questions. Considerations for choosing a beamline include beam energy, Q range, data resolution, and collection time. Powder patterns generated from our detailed single crystal X-ray diffraction work on the homologous series indicate peak overlap, peak splitting, and a wide range of peak intensity in the most helpful/indicative peaks. For example, Figure 2 shows the most indicative peaks for phase identification are less than 2% of the maximum peaks. Additionally, from our experience with bulk laboratory synthesis we know that it is common to have multiple members of the series in one synthetic batch. Therefore, high resolution data is necessary to deconvolute split peaks and visualize low angle and low intensity indicative peaks. Although the fast collection time at 17-BM (seconds as compared to 30 min^{-1} h at 11-BM) and high energy at 11-ID-C (105 keV) coupled with the fast collection time would have been advantageous for highly absorbing samples, the collapsing of Q space that occurs with higher energies would put the low angle peaks in the beam stop, blocking some of the most important peaks for phase identification of this homologous series. The point detectors combined with Si(111) analyzer crystals at 11-BM provide low background, where no back scattering, fluorescence, or additional signal from the sample environment interfere with the pattern, provide the necessary resolution to see peak splitting and peak shapes to deconvolute the related phases. It would be ideal to have a beamline with higher energy than 11-BM's current range (e.g., >50 keV to avoid the Sn absorption edge) and a collection time of 2 or 3 min instead of 30−60 min coupled with the high resolution detectors. However, 11-BM is the best beamline available for this work due to the low background and high data resolution.

Question 2: Is Your Sample Too Absorbing? Calculate the X-ray absorption of your starting material using the Cromer and Liberman algorithm (https://11bm.xray.aps.anl.gov/absorb/absorb.php).[41] Single crystals of $Ce_6Co_5Ge_{16}$ and $Ce_7Co_6Ge_{19}$ were grown in a Sn flux consisting of about 1/3 of the starting material which would cause absorption issues for an in situ experiment.[38,39] Therefore, the amount of Sn in the reactions was reduced and the energy of the beamline was shifted to 27 keV to avoid the Sn absorption edge of ∼30 keV.

Question 2.1: What Type of Reaction Vessel Should You Use? Heavily absorbing samples will require small reaction capillaries (1 mm o.d.) to decrease absorption while less absorbing materials may require larger diameter capillaries. Smaller capillaries can be used, but challenges such as difficulty loading samples, surface effects, capillary action, and an increased likelihood to breaking should be considered. Kapton capillaries are best for use in temperature ranges up to 400 °C. For the work on the homologous series, a reaction vessel that is transparent to X-rays, can withstand 1100 °C for greater than 48 h, is nonreactive with the starting materials, and provides an inert atmosphere to prevent oxidation was required. Two options following these criteria are sapphire (maximum temperature ∼ 2000 °C) and fused silica tubes (maximum temperature ∼ 1150 °C); the latter were chosen due to the cost and no additional benefit from sapphire.

Question 2.2: Does Your Sample Need to Be Diluted? The packing density can be decreased by diluting the sample. A material with low X-ray absorption and without unwanted diffraction, such as an inert and stable standard or ground silica wool, are ideal options. We diluted the sample with ground silica wool to mitigate absorption issues and provide more nucleation sites to encourage random orientation and smaller crystal sizes. Additionally, bigger grains/single crystals cause issues in both area detectors and point detectors. Because 11-BM uses a point detector (instead of an area detector), the data is only a small slice of the diffraction ring which makes reducing the contribution of crystallites more of a priority.

Question 3: What Starting Material Will You Use? Preliminary synthesis attempts used elemental Ce, Co, Ge, and Sn as starting material in an attempt to avoid local minima barriers of formed binary compounds. Therefore, the in situ reactions utilized elemental Ce, Co, Ge, and Sn. Other starting materials include binary, ternary, and arc-melted precursors. For more information on growth techniques, please refer to previous work.[25,30,35,42,43]

Question 4: What Is the Morphology of Your Starting Material? Metal rods and chunks were used in the initial large

https://doi.org/10.1021/acs.chemmater.1c02413
Chem. Mater. 2021, 33, 7657−7664

scale reactions.[38,39] However, fine powders of each element were ideal for in situ studies due to the increased surface area for reactivity and ease of packing into small (<1 mm) capillaries. It is important to note that certain elements (such as Ce) will become more air sensitive as the particle size decreases. Handle with caution.

Question 5: Will Your Reactants Become Molten? If the answer is "no", then the default orientation of the beamline will suffice. However, if the answer is "yes", a vertical orientation will be necessary to keep the liquidous sample from moving out of the beam. Horizontal orientations are problematic for syntheses where the low melting flux has a low viscosity. For example, when using a Sn flux in a horizontal orientation, at temperatures above 250 °C, the sample would flow in the sample capillary out of the X-ray beam since it is nearly impossible to ensure a completely level horizontal orientation. Therefore, a vertical orientation is ideal to monitor the in situ flux growth of complex intermetallic materials, such as the $Ce_{n+1}Co_nGe_{3n+1}$ homologous series.

Question 6: Is a Specific Atmosphere Required? Is an Inert Atmosphere Necessary? If an inert atmosphere is necessary, starting materials will need to be packed into a capillary in an inert atmosphere (i.e., glovebox or glovebag) and sealed with an appropriate epoxy. The epoxy side will be at the top of the vertical sample environment and therefore far enough away from the heating element to prevent melting. We packed fused silica tubes (0.9 mm o.d.) with starting materials in an Ar atm glovebox and sealed with 2-part epoxy. It is important to note that multiple capillaries should be prepared for each reaction due to the thin capillary walls breaking easily.

Question 7: What Is Your Proposed Heating Profile? The proposed synthetic conditions should be determined with consideration of the awarded amount of time at the beam. Additionally, it should be based on preliminary reaction conditions. The heating method used will greatly depend on the maximum temperature necessary for the reaction. For additional information regarding how heating profiles are determined, see refs 25, 30, 31, 35, 44, and 45. Figure 3 provides a checklist to prepare for beam time.

From our previous considerations, we can highlight 5 main obstacles that need to be addressed in a furnace design.

Obstacle 1. Previous synthetic attempts were focused on growing single crystals; however, crystallite formation, particularly the plate-like crystals of the homologous series, can lead to preferred orientation causing variation of peak intensity. Preferred orientation is more an issue when using a point detector as compared to an area detector because the diffraction pattern is only from a slice of the diffraction ring; therefore, the intensity variations will be more pronounced. Additionally, preferred orientation can also become a problem. Therefore, the sample needs to be spun.

Obstacle 2. The starting materials are highly absorbing. Reaction ratios have been modified to reduce absorption, but a small (1 mm o.d.) capillary is still required. The sample environment must couple to capillaries this size.

Obstacle 3. The reactants become molten during the heating profile; therefore, the sample environment and furnace need to be in a vertical orientation to prevent the sample from flowing out of the beam.

Obstacle 4. The starting materials are air sensitive; therefore, the samples need to be packed in an inert atmosphere. Additionally, the samples need to be heated in an inert atmosphere, so a closed environment is required.

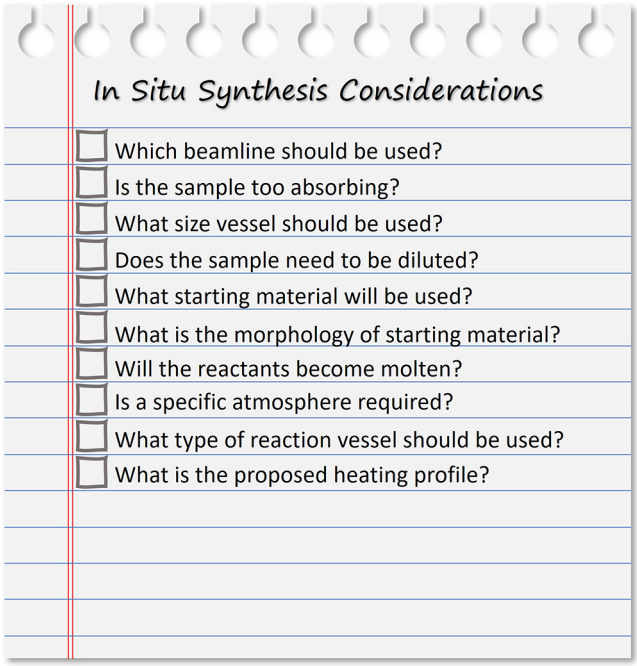

Figure 3. Checklist of questions to consider when preparing in situ synthesis diffraction experiments at a synchrotron facility.

Obstacle 5. The starting materials have high melting points, even with the use of a low melting flux. Therefore, the proposed heating profile requires the samples to be held at 1000 or 1100 °C for ∼ 2 days, which requires robust heating elements and appropriate insulation.

THE FINAL DESIGN

The overall sample environment, shown in Figure 4, was designed to perform in situ synthesis reactions in a synchrotron beam, specifically at 11-BM of the Advanced Photon Source at Argonne National Laboratory. Table S1 provides a list of components used in the overall design. A detailed description of the assembly can be found in the Supporting Information.

Obstacle 1—Solution. To reduce the preferred orientation, a spinning attachment was incorporated. The use of quartz wool as an inert standard can serve to randomize crystallite orientation as well.

Obstacle 2—Solution. The starting material was mixed with quartz wool before packed into the capillary to decrease the amount of absorbing material in the capillary.

Obstacle 3—Solution. A 1/16 in. Swagelok straight fitting was modified to couple to the motor head, which allowed for the sample to hang vertically from the motor head. The bottom piece is a 1/16 in. compression fitting that snugly holds the capillary in place. The top piece was machined to fit the 5 mm rotating motor head which is held in place by two set screws. The motor/capillary configuration was coupled, via cage assembly rods, to a flow cell cage with a universal base plate.

Obstacle 4—Solution. A 1 mm o.d. capillary, flame-sealed on one end, was packed in an Ar atmosphere glovebox, and the top end is sealed with a 2-part epoxy. The epoxy end is placed in the modified Swagelok piece to keep the epoxy as far from the heat source as possible to prevent it from melting.

Obstacle 5—Solution. Most solid state reactions occur at temperatures of 700−1300 °C.[30] To grow members of the

https://doi.org/10.1021/acs.chemmater.1c02413
Chem. Mater. 2021, 33, 7657−7664

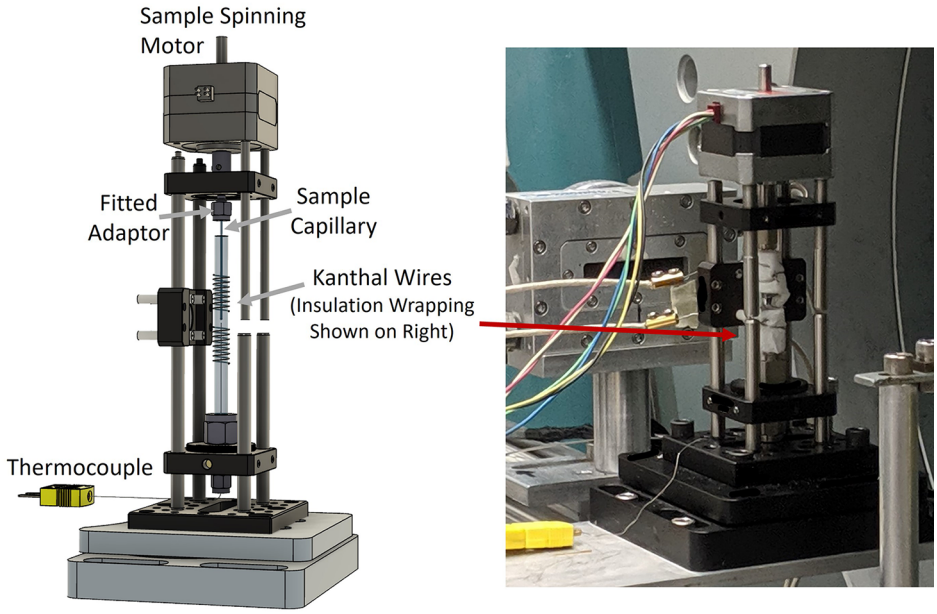

Figure 4. Schematic (left) and image (right) of the furnace apparatus. The insulation has been omitted in the schematic for clarity.

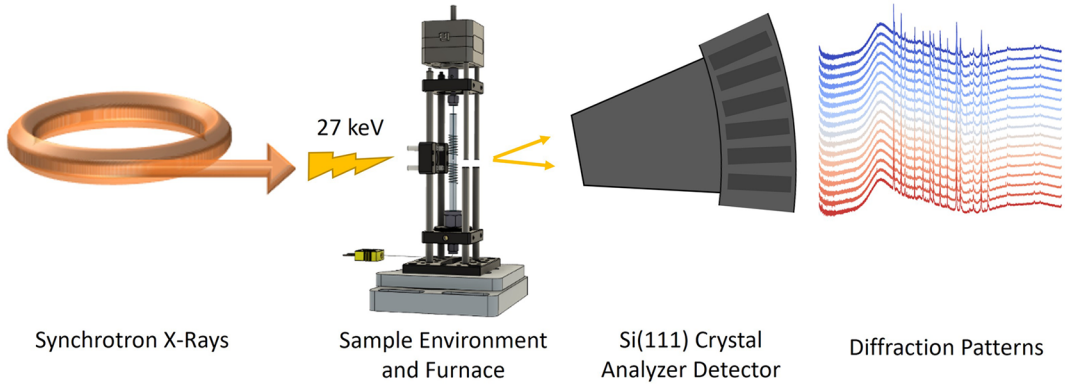

Figure 5. General schematic for the in situ monitoring of intermetallic synthesis. Synchrotron radiation is generated and focused at 11-BM. The X-rays pass through the sample environment and diffraction data is collected on the Si crystal analyzer detector. The resulting powder patterns are compiled, and phase determination and evolution are evaluated by the Rietveld method.

intermetallic homologous series, $Ce_{n+1}Co_nGe_{3n+1}$, a maximum operating temperature of 1100 °C is necessary. In our initial experiments, reaction conditions were modified to limit the dwell time to no longer than 48 h. However, including the ramp up time and ramp down time, this heating apparatus needed to be robust at high temperatures for long periods of time without blocking diffraction rays and generating additional unwanted diffraction. The versatile flow cell[46] utilizes two Kanthal A-1 resistive wires wrapped around ceramic rods with the sample placed between them. These furnaces are well-known to go up to a maximum of 1050 °C but not for as long as required (48 h) and not the required 1100 °C, which is in part due to heat loss in all directions. Kanthal A-1 wire has a melting point of 1400 °C, and the loss of heat in all directions requires the wire to heat above 1400 °C to keep the sample at the required temperature. To extend the working temperature range of the resistive coils, the sample was placed in the center of the coil for homogeneous heat treatment. The coils, wrapped around a 6 mm o.d. fused silica tube, were wrapped in insulation to reduce heat loss. A small section of insulation was removed from both sides, using tweezers, to allow for the beam to pass through. A thermocouple was placed near the bottom of the sample to allow for a temperature feedback loop. Practice trials reached the desired temperature of 1100 °C and lasted there for over 3 days. A platinum wire heating element and sapphire tubing can be used for a higher temperature range.

VALIDATION STUDY

Elemental powders of Ce, Co, Ge, and Sn were combined in an Ar atmosphere glovebox, ground with quartz wool, and packed in a fused silica capillary (0.9 mm o.d.) that had been flame-sealed on one side. The open end was sealed using 2-part epoxy and left to dry for 1−2 h as drying times are much longer inside a glovebox. The capillary was removed from the glovebox, connected to the motor via the fitted adaptor, and then *carefully* lowered into the fused silica tube wrapped by the resistive furnace. Care must be taken at this point to ensure the reaction capillary does not break. Adjustments of the wires and mullite rods may be necessary to center the sample capillary in the insulation gap. The sample was then aligned in the beam (first calibrated using a NIST LaB_6 standard), and the

https://doi.org/10.1021/acs.chemmater.1c02413
Chem. Mater. 2021, 33, 7657−7664

programmable temperature controller is set to the desired heating profile. Scans are collected throughout the reaction to monitor crystallization and structure formation. Figure 5 shows a general schematic for the in situ synthetic process. Resulting powder patterns can be analyzed by the Rietveld method in various software packages, such as GSAS-II[47] or TOPAS.[48] In this work, a crash cool method was employed but the apparatus can also accommodate controlled cooling. For reactions with lengthy reaction times, multiple cell synthesis can be completed with multiple reactions running at the same time.

DATA ANALYSIS

The first step in data analysis occurs during the collection process by generating waterfall plots to visually check the powder patterns as they are collected. The melting temperatures of the starting materials should be monitored to ensure the feedback loop is providing a correct temperature read out. Important events, such as melting and formation of phases, can be visually identified with more ease when compared directly in the waterfall plot. Phase identification can be done by simple peak matching or by more detailed analysis with Rietveld refinements.

Once you identify the important areas of the data collection you can delve in to identifying each phase. Figure 6 shows an example waterfall plot from the heating of a Ce−Co−Ge−Sn reaction vessel. Critical events are highlighted at 290, 570, 820, and 960 °C. Although no reaction intermediates were formed during this synthesis, the waterfall plot can be helpful in designing synthetic conditions to isolate intermediate phases.[1,15] A simple visualization software will provide a wealth of information about the critical events in your sample.

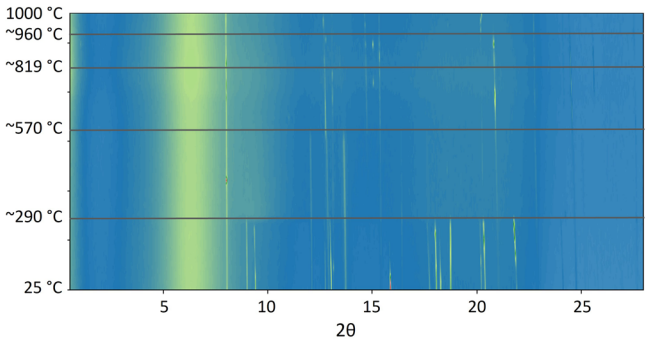

Figure 6. Waterfall plot/contour map compiled of 56 synchrotron powder diffraction patterns from a sample of Ce−Co−Ge−Sn heating from 25 to 1000 °C at a rate of 1.67 °C/min where λ = 0.4592 Å. Horizontal lines are superimposed to bring attention to the appearance and disappearance of a phase.

OUTLOOK

A new sample environment and in situ method that can monitor solid state reactions, specifically those targeting intermetallic phases and utilizing a metal flux, have been designed, implemented, and presented. Spinning the sample capillary decreases preferred orientation and provides sample mixing. Mixing highly absorbing samples with an inert material both mitigates the absorption issue and provides a multitude of nucleation sites. To keep the molten sample fully engulfed in the beam, the sample environment is designed for a vertical sample orientation. Air sensitive samples and samples that require a specific atmosphere can be accommodated by the apparatus by sealing the capillary under inert atmosphere or connecting to a gas flow cell. Resistive heating elements consisting of Kanthal or Pt wires provide temperatures up to at least 1100 °C for >40 h and 1000 °C for >60 h which is necessary for high melting intermetallic phases. All parts can be purchased commercially, and only three need to be modified from their original form, which can be easily done with simple machining. This design has proved to be a pivotal tool in the in situ monitoring of metal flux growth of intermetallics at 11-BM. This method provides a more accessible and streamlined avenue to the in situ monitoring of intermetallic phase formation and can revolutionize how new intermetallic reactions are designed.

ASSOCIATED CONTENT

Supporting Information

The Supporting Information is available free of charge at https://pubs.acs.org/doi/10.1021/acs.chemmater.1c02413.

Preliminary furnace design, assembly information, and detailed schematics of each aspect of the apparatus (PDF)

AUTHOR INFORMATION

Corresponding Authors

Saul H. Lapidus − *X-ray Science Division, Advanced Photon Source, Argonne National Laboratory, Argonne, Illinois 60439, United States;* orcid.org/0000-0002-7486-4325; Email: slapidus@anl.gov

Julia Y. Chan − *Department of Chemistry & Biochemistry, University of Texas at Dallas, Richardson, Texas 75080, United States;* orcid.org/0000-0003-4434-2160; Email: julia.chan@utdallas.edu

Authors

Ashley Weiland − *Department of Chemistry & Biochemistry, University of Texas at Dallas, Richardson, Texas 75080, United States;* orcid.org/0000-0001-7198-3559

Matthew G. Frith − *X-ray Science Division, Advanced Photon Source, Argonne National Laboratory, Argonne, Illinois 60439, United States;* orcid.org/0000-0002-9169-7434

Complete contact information is available at: https://pubs.acs.org/10.1021/acs.chemmater.1c02413

Notes

The authors declare no competing financial interest.

ACKNOWLEDGMENTS

This material is based upon work supported by the U.S. Department of Energy, Office of Science, Office of Workforce Development for Teachers and Scientists, Office of Science Graduate Student Research (SCGSR) program. The SCGSR program is administered by the Oak Ridge Institute for Science and Education for the DOE under Contract No. DE-SC0014664. J.Y.C. gratefully acknowledges National Science Foundation Grant No. DMR-1700030 for support of this project. A.W. acknowledges the support of the Eugene McDermott Graduate Fellows Program. This research used resources of the Advanced Photon Source, a U.S. Department of Energy (DOE) Office of Science User Facility, operated for the DOE Office of Science by Argonne National Laboratory under Contract No. DE-AC02-06CH11357.

REFERENCES

(1) Shoemaker, D. P.; Hu, Y.-J.; Chung, D. Y.; Halder, G. J.; Chupas, P. J.; Soderholm, L.; Mitchell, J. F.; Kanatzidis, M. G. In Situ Studies of a Platform for Metastable Inorganic Crystal Growth and Materials Discovery. *Proc. Natl. Acad. Sci. U. S. A.* **2014**, *111*, 10922−10927.

(2) Yin, L.; Murphy, M.; Kim, K.; Hu, L.; Cabana, J.; Siegel, D. J.; Lapidus, S. H. Synthesis of Antiperovskite Solid Electrolytes: Comparing Li_3SI, Na_3SI, and Ag_3SI. *Inorg. Chem.* **2020**, *59*, 11244−11247.

(3) Bai, J.; Sun, W.; Zhao, J.; Wang, D.; Xiao, P.; Ko, J. Y. P.; Huq, A.; Ceder, G.; Wang, F. Kinetic Pathways Templated by Low-Temperature Intermediates During Solid-State Synthesis of Layered Oxides. *Chem. Mater.* **2020**, *32*, 9906−9913.

(4) Pienack, N.; Bensch, W. In-Situ Monitoring of the Formation of Crystalline Solids. *Angew. Chem., Int. Ed.* **2011**, *50*, 2014−2034.

(5) Zevalkink, A.; Smiadak, D. M.; Blackburn, J. L.; Ferguson, A. J.; Chabinyc, M. L.; Delaire, O.; Wang, J.; Kovnir, K.; Martin, J.; Schelhas, L. T.; Sparks, T. D.; Kang, S. D.; Dylla, M. T.; Snyder, G. J.; Ortiz, B. R.; Toberer, E. S. A Practical Field Guide to Thermoelectrics: Fundamentals, Synthesis, and Characterization. *Appl. Phys. Rev.* **2018**, *5*, No. 021303.

(6) Chen, B.-R.; Sun, W.; Kitchaev, D. A.; Mangum, J. S.; Thampy, V.; Garten, L. M.; Ginley, D. S.; Gorman, B. P.; Stone, K. H.; Ceder, G.; Toney, M. F.; Schelhas, L. T. Understanding Crystallization Pathways Leading to Manganese Oxide Polymorph Formation. *Nat. Commun.* **2018**, *9*, 2553.

(7) Moorhouse, S. J.; Wu, Y.; Buckley, H. C.; O'Hare, D. Time-Resolved *in situ* Powder X-ray Diffraction Reveals the Mechanisms of Molten Salt Synthesis. *Chem. Commun.* **2016**, *52*, 13865−13868.

(8) Kanatzidis, M. G. Discovery-Synthesis, Design, and Prediction of Chalcogenide Phases. *Inorg. Chem.* **2017**, *56*, 3158−3173.

(9) Luo, J.; Martinez-Casado, F. J.; Balmes, O.; Yang, J.; Persson, C.; Engqvist, H.; Xia, W. In Situ Synchrotron X-ray Diffraction Analysis of the Setting Process of Brushite Cement: Reaction and Crystal Growth. *ACS Appl. Mater. Interfaces* **2017**, *9*, 36392−36399.

(10) Abeysinghe, D.; Huq, A.; Yeon, J.; Smith, M. D.; zur Loye, H.-C. In Situ Neutron Diffraction Studies of the Flux Crystal Growth of the Reduced Molybdates $La_4Mo_2O_{11}$ and $Ce_4Mo_2O_{11}$: Revealing Unexpected Mixed-Valent Transient Intermediates and Determining the Sequence of Events during Crystal Growth. *Chem. Mater.* **2018**, *30*, 1187−1197.

(11) Bianchini, M.; Fauth, F.; Hartmann, P.; Brezesinski, T.; Janek, J. An In Situ Structural Study on the Synthesis and Decomposition of $LiNiO_2$. *J. Mater. Chem. A* **2020**, *8*, 1808−1820.

(12) Sommer, S.; Bøjesen, E. D.; Reardon, H.; Iversen, B. B. Atomic Scale Design of Spinel $ZnAl_2O_4$ Nanocrystal Synthesis. *Cryst. Growth Des.* **2020**, *20*, 1789−1799.

(13) Gvozdetskyi, V.; Owens-Baird, B.; Hong, S.; Cox, T.; Bhaskar, G.; Harmer, C.; Sun, Y.; Zhang, F.; Wang, C.-Z.; Ho, K.-M.; Zaikina, J. V. From $NaZn_4Sb_3$ to HT-$Na_{1-x}Zn_{4-y}Sb_3$: Panoramic Hydride Synthesis, Structural Diversity, and Thermoelectric Properties. *Chem. Mater.* **2019**, *31*, 8695−8707.

(14) Paradis-Fortin, L.; Lemoine, P.; Prestipino, C.; Kumar, V. P.; Raveau, B.; Nassif, V.; Cordier, S.; Guilmeau, E. Time-Resolved In Situ Neutron Diffraction Study of $Cu_{22}Fe_8Ge_4S_{32}$ Germanite: A Guide for the Synthesis of Complex Chalcogenides. *Chem. Mater.* **2020**, *32*, 8993−9000.

(15) Vasquez, G.; Huq, A.; Latturner, S. E. In Situ Neutron Diffraction Studies of the Metal Flux Growth of Ba/Yb/Mg/Si Intermetallics. *Inorg. Chem.* **2019**, *58*, 8111−8119.

(16) Oezaslan, M.; Hasché, F.; Strasser, P. In Situ Observation of Bimetallic Alloy Nanoparticle Formation and Growth Using High-Temperature XRD. *Chem. Mater.* **2011**, *23*, 2159−2165.

(17) Beck, A.; Huang, X.; Artiglia, L.; Zabilskiy, M.; Wang, X.; Rzepka, P.; Palagin, D.; Willinger, M.-G.; van Bokhoven, J. A. The Dynamics of Overlayer Formation on Catalyst Nanoparticles and Strong Metal-support Interaction. *Nat. Commun.* **2020**, *11*, 3220.

(18) Yu, S.-H.; Huang, X.; Brock, J. D.; Abruña, H. D. Regulating Key Variables and Visualizing Lithium Dendrite Growth: An *Operando* X-ray Study. *J. Am. Chem. Soc.* **2019**, *141*, 8441−8449.

(19) Li, Q.; Li, H.; Xia, Q.; Hu, Z.; Zhu, Y.; Yan, S.; Ge, C.; Zhang, Q.; Wang, X.; Shang, X.; Fan, S.; Long, Y.; Gu, L.; Miao, G.-X.; Yu, G.; Moodera, J. S. Extra Storage Capacity in Transition Metal Oxide Lithium-Ion Batteries Revealed by in situ Magnetometry. *Nat. Mater.* **2021**, *20*, 76−83.

(20) Clancy, M.; Styles, M. J.; Bettles, C. J.; Birbilis, N.; Chen, M.; Zhang, Y.; Gu, Q.; Kimpton, J. A.; Webster, N. A. S. *In Situ* Synchrotron X-Ray Diffraction Investigation of the Evolution of a $PbO_2/PbSO_4$ Surface Layer on a Copper Electrowinning Pb Anode in a Novel Electrochemical Flow Cell. *J. Synchrotron Radiat.* **2015**, *22*, 366−375.

(21) Liu, R.; Ulbrandt, J. G.; Hsing, H.-C.; Gura, A.; Bein, B.; Sun, A.; Pan, C.; Bertino, G.; Lai, A.; Cheng, K.; Doyle, E.; Evans-Lutterodt, K.; Headrick, R. L.; Dawber, M. Role of Ferroelectric Polarization During Growth of Highly Strained Ferroelectric Materials. *Nat. Commun.* **2020**, *11*, 2630.

(22) Rabol Jorgensen, L.; Moeslund Zeuthen, C.; Andersen Borup, K.; Roelsgaard, M.; Lau Nyborg Broge, N.; Beyer, J.; Brummerstedt Iversen, B. Operando X-ray Scattering Study of Thermoelectric β-Zn_4Sb_3. *IUCrJ* **2020**, *7*, 100−104.

(23) Xiong, Y.; Yang, Y.; Joress, H.; Padgett, E.; Gupta, U.; Yarlagadda, V.; Agyeman-Budu, D. N.; Huang, X.; Moylan, T. E.; Zeng, R.; Kongkanand, A.; Escobedo, F. A.; Brock, J. D.; DiSalvo, F. J.; Muller, D. A.; Abruña, H. D. Revealing the Atomic Ordering of Binary Intermetallics using in situ Heating Techniques at Multilength Scales. *Proc. Natl. Acad. Sci. U. S. A.* **2019**, *116*, 1974.

(24) DiSalvo, F. J. Solid-State Chemistry: A Rediscovered Chemical Frontier. *Science* **1990**, *247*, 649−655.

(25) Canfield, P. C.; Fisk, Z. Growth of Single Crystals From Metallic Fluxes. *Philos. Mag. B* **1992**, *65*, 1117−1123.

(26) Canfield, P. C.; Fisher, I. R. High-Temperature Solution Growth of Intermetallic Single Crystals and Quasicrystals. *J. Cryst. Growth* **2001**, *225*, 155−161.

(27) National Research Council. *Frontiers in Crystalline Matter: From Discovery to Technology*; The National Academies Press: 2009.

(28) Phelan, W. A.; Menard, M. C.; Kangas, M. J.; McCandless, G. T.; Drake, B. L.; Chan, J. Y. Adventures in Crystal Growth: Synthesis and Characterization of Single Crystals of Complex Intermetallic Compounds. *Chem. Mater.* **2012**, *24*, 409−420.

(29) Schmitt, D. C.; Drake, B. L.; McCandless, G. T.; Chan, J. Y. Targeted Crystal Growth of Rare Earth Intermetallics with Synergistic Magnetic and Electrical Properties: Structural Complexity to Simplicity. *Acc. Chem. Res.* **2015**, *48*, 612−618.

(30) Tachibana, M. *Beginners Guide to Flux Crystal Growth*; Springer: 2017.

(31) Canfield, P. C. New Materials Physics. *Rep. Prog. Phys.* **2020**, *83*, No. 016501.

(32) Cordova, D. L. M.; Johnson, D. C. Synthesis of Metastable Inorganic Solids with Extended Structures. *ChemPhysChem* **2020**, *21*, 1345−1368.

(33) Kovnir, K. Predictive Synthesis. *Chem. Mater.* **2021**, *33*, 4835−4841.

(34) Fisk, Z.; Remeika, J. P. Growth of Single Crystals From Molten Metal Fluxes. In *Handbook on the Physics and Chemistry of Rare Earths*; Elsevier: 1989; Vol. *12*, pp 53−70.

(35) Kanatzidis, M. G.; Pöttgen, R.; Jeitschko, W. The Metal Flux: A Preparative Tool for the Exploration of Intermetallic Compounds. *Angew. Chem., Int. Ed.* **2005**, *44*, 6996−7023.

(36) Samarth, N. Quantum Materials Discovery From A Synthesis Perspective. *Nat. Mater.* **2017**, *16*, 1068.

(37) Weiland, A.; Felder, J. B.; McCandless, G. T.; Chan, J. Y. One Ce, Two Ce, Three Ce, Four? An Intermetallic Homologous Series to Explore: $A_{n+1}B_nX_{3n+1}$. *Chem. Mater.* **2020**, *32*, 1575−1580.

(38) Felder, J. B.; Weiland, A.; Hodovanets, H.; McCandless, G. T.; Estrada, T. G.; Martin, T. J.; Walker, A. V.; Paglione, J.; Chan, J. Y.

https://doi.org/10.1021/acs.chemmater.1c02413
Chem. Mater. 2021, 33, 7657−7664

Law and Disorder: Special Stacking Units—Building the Intergrowth $Ce_6Co_5Ge_{16}$. *Inorg. Chem.* **2019**, *58*, 6037−6043.
(39) Weiland, A.; Wei, K.; McCandless, G. T.; Felder, J. B.; Eddy, L. J.; Baumbach, R. E.; Chan, J. Y. Strongly Correlated Electron Behavior in a New Member of the $A_{n+1}B_nX_{3n+1}$ Homologous Series: $Ce_7Co_6Ge_{19}$. *Phys. Rev. Mater.* **2020**, *4*, No. 074408.
(40) Wang, J.; Toby, B. H.; Lee, P. L.; Ribaud, L.; Antao, S. M.; Kurtz, C.; Ramanathan, M.; Von Dreele, R. B.; Beno, M. A. A Dedicated Powder Diffraction Beamline at the Advanced Photon Source: Commissioning and Early Operational Results. *Rev. Sci. Instrum.* **2008**, *79*, No. 085105.
(41) Cromer, D. T.; Liberman, D. A. Anomalous Dispersion Calculations Near to and on the Long-Wavelength Side of an Absorption Edge. *Acta Crystallogr., Sect. A: Cryst. Phys., Diffr., Theor. Gen. Crystallogr.* **1981**, *37*, 267−268.
(42) Canfield, P. C. Fishing the Fermi Sea. *Nat. Phys.* **2008**, *4*, 167−169.
(43) Sun, W.; Dacek, S. T.; Ong, S. P.; Hautier, G.; Jain, A.; Richards, W. D.; Gamst, A. C.; Persson, K. A.; Ceder, G. The Thermodynamic Scale of Inorganic Crystalline Metastability. *Sci. Adv.* **2016**, *2*, e1600225.
(44) Janssen, Y.; Angst, M.; Dennis, K. W.; McCallum, R. W.; Canfield, P. C. Differential Thermal Analysis and Solution Growth of Intermetallic Compounds. *J. Cryst. Growth* **2005**, *285*, 670−680.
(45) De Yoreo, J.; Mandrus, D.; Soderholm, L.; Forbes, T.; Kanatzidis, M.; Erlebacher, J.; Laskin, J.; Wiesner, U.; Xu, T.; Billinge, S. *Basic Research Needs Workshop on Synthesis Science for Energy Relevant Technology*; USDOE Office of Science (SC): 2016.
(46) Chupas, P. J.; Chapman, K. W.; Kurtz, C.; Hanson, J. C.; Lee, P. L.; Grey, C. P. A Versatile Sample-Environment Cell for Non-Ambient X-ray Scattering Experiments. *J. Appl. Crystallogr.* **2008**, *41*, 822−824.
(47) Toby, B. H.; Von Dreele, R. B. GSAS-II: The Genesis of a Modern Open-Source All Purpose Crystallography Software Package. *J. Appl. Crystallogr.* **2013**, *46*, 544−549.
(48) Coelho, A. TOPAS and TOPAS-Academic: An Optimization Program Integrating Computer Algebra and Crystallographic Objects Written in C++. *J. Appl. Crystallogr.* **2018**, *51*, 210−218.

https://doi.org/10.1021/acs.chemmater.1c02413
Chem. Mater. 2021, 33, 7657−7664